

# Twin-field quantum key distribution without phase locking

Wei Li,<sup>1,2,\*</sup> Likang Zhang,<sup>1,2,\*</sup> Yichen Lu,<sup>1,2,\*</sup> Zheng-Ping Li,<sup>1,2,3</sup> Cong Jiang,<sup>4</sup> Yang Liu,<sup>4</sup> Jia Huang,<sup>5</sup> Hao Li,<sup>5</sup> Zhen Wang,<sup>5</sup> Xiang-Bin Wang,<sup>3,4,6</sup> Qiang Zhang,<sup>1,2,3,4</sup> Lixing You,<sup>5</sup> Feihu Xu,<sup>1,2,3</sup> and Jian-Wei Pan<sup>1,2,3</sup>

<sup>1</sup>*Hefei National Research Center for Physical Sciences  
at the Microscale and School of Physical Sciences,*

*University of Science and Technology of China, Hefei 230026, China*

<sup>2</sup>*Shanghai Research Center for Quantum Science and CAS Center  
for Excellence in Quantum Information and Quantum Physics,  
University of Science and Technology of China, Shanghai 201315, China*

<sup>3</sup>*Hefei National Laboratory, University of Science  
and Technology of China, Hefei 230088, China*

<sup>4</sup>*Jinan Institute of Quantum Technology, Jinan, Shandong 250101, China*

<sup>5</sup>*State Key Laboratory of Functional Materials for Informatics,  
Shanghai Institute of Microsystem and Information Technology,  
Chinese Academy of Sciences, Shanghai 200050, China*

<sup>6</sup>*State Key Laboratory of Low Dimensional Quantum Physics,  
Department of Physics, Tsinghua University, Beijing, China*

## Abstract

Twin-field quantum key distribution (TF-QKD) has emerged as a promising solution for practical quantum communication over long-haul fiber. However, previous demonstrations on TF-QKD require the phase locking technique to coherently control the twin light fields, inevitably complicating the system with extra fiber channels and peripheral hardware. Here we propose and demonstrate an approach to recover the single-photon interference pattern and realize TF-QKD *without* phase locking. Our approach separates the communication time into reference frames and quantum frames, where the reference frames serve as a flexible scheme for establishing the global phase reference. To do so, we develop a tailored algorithm based on fast Fourier transform to efficiently reconcile the phase reference via data post-processing. We demonstrate no-phase-locking TF-QKD from short to long distances over standard optical fibers. At 50-km standard fiber, we produce a high secret key rate (SKR) of 1.27 Mbit/s, while at 504-km standard fiber, we obtain the repeater-like key rate scaling with a SKR of 34 times higher than the repeaterless secret key capacity. Our work provides a scalable and practical solution to TF-QKD, thus representing an important step towards its wide applications.

*Introduction.*—Quantum key distribution (QKD) can provide information-theoretically secure keys among distant parties [1] and it has become an indispensable cryptographic primitive in the upcoming quantum era [2, 3]. Due to the loss of photons in their transmission, the point-to-point secret key capacity ( $\text{SKC}_0$ ) without the quantum repeater scales linearly  $O(\eta)$  with the channel transmission [4–6]. The twin-field (TF) QKD protocol [7], an efficient version of measurement-device-independent QKD [8], can greatly enhance the transmission distance by achieving a repeater-like rate-loss scaling of  $O(\sqrt{\eta})$  with current available technology. Consequently, TF-QKD has been studied extensively in theory [9–12] and experiment [13–21]. These efforts make the long-haul fiber network within reach. Moreover, its measurement-device-independent advantage can remove trusted nodes from the networks, thus granting a security boost over deployed quantum communication network [22–24].

In practice, however, TF-QKD is phase-sensitive [7], which normally requires sufficiently long coherence time for two independent laser sources. In previous TF-QKD realizations,

---

\* Equal contribution.

such stringent requirement has been fulfilled by phase-locking laser sources using the optical phase-lock loop [13, 15, 18, 21], the time-frequency dissemination [14, 19, 20] or the injection locking [16] techniques. These approaches require extra servo channels to disseminate the reference light and peripheral hardware to perform the locking, which could potentially hinder the wide deployment of TF-QKD in network settings. Furthermore, the future quantum network may involve users with free-space link [25, 26] or with integrated photonic chip [27–29]. However, the servo channel is hard to establish in the free-space link, and the phase-locking components are challenging to be integrated on chip.

In this work, we propose and demonstrate an approach to realize TF-QKD *without* phase locking. We alternate the communication period into quantum frame (Q-frame) and reference frame (R-frame), and use the R-frame to provide a phase reference for the Q-frame by reconciling the signals via data post-processing. We develop an algorithm based on the fast Fourier transform (FFT) to efficiently track the frequency and the phase fluctuation. By doing so, we are able to recover the interference pattern with 259 photon detections in a duration of 7  $\mu\text{s}$ , yielding an interference error rate (ER) of 2.32%, or an ER of 3.74% with 159 photon detections in a duration of 11  $\mu\text{s}$ . Moreover, we derive an analytical model to study the sources of phase fluctuation and provide a guideline to optimize the experimental parameters in the aspect of the ratio of the Q-frame to the R-frame. To test our approach, we build a TF-QKD setup without any phase locking (or phase compensating) at the transmitter (or receiver), and demonstrate TF-QKD from 50- to 504-km standard fiber channels. A secret key rate (SKR) of 2.05 bit/s is generated over 504-km standard fiber (96.8 dB loss or equivalent to 605-km ultra low loss fiber) in the finite-size regime, which is 34 times higher than SKC<sub>0</sub>. At 50-km standard fiber, we are able to produce 1.27 Mbit/s secret keys.

*No-phase-locking scheme.*—The phase difference of two light fields  $\Phi(t)$  evolves as,

$$\Phi(t) = 2\pi\nu t + \phi_0 + \Delta\phi(t), \quad (1)$$

where  $\nu$ ,  $\phi_0$  and  $\Delta\phi(t)$  denote the beat-note frequency, the initial phase and the phase fluctuation respectively. Both  $\nu$  and  $\phi_0$  can be estimated via the data post-processing, whereas  $\Delta\phi(t)$  includes the intrinsic phase noise of the laser sources and the fluctuation introduced in the channel transmission.

To perform the parameter estimation, we propose to supplement the quantum pulses

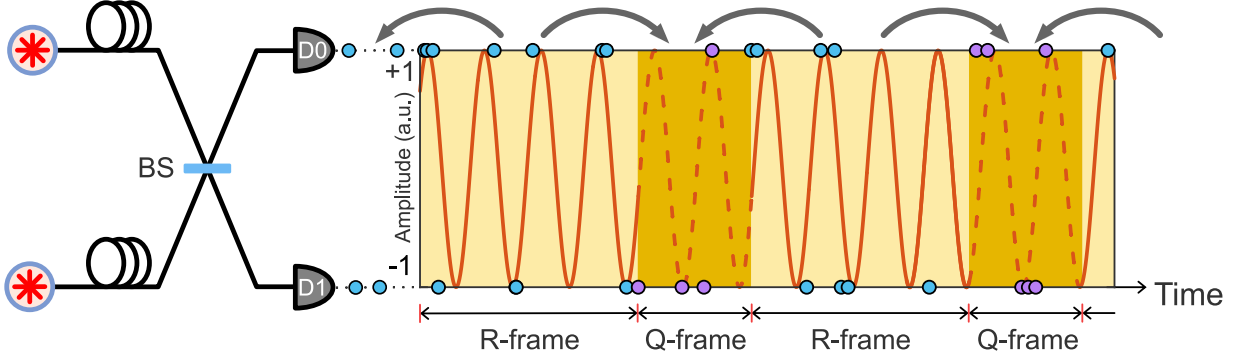


FIG. 1. No-phase-locking scheme. The interference pattern is evaluated frequently in the R-frame, providing a phase reference for the Q-frame. The detection events of  $D_0$  ( $D_1$ ) are mapped to the amplitude of  $+1$  ( $-1$ ) and the detection probability is related to the interference pattern.

(Q-frame) with strong R-frame. The R-frame is used to reconcile the phase in the Q-frame through post-processing the photon detection events. As shown in Fig. 1, the detection probabilities of two detectors are correlated with the interference pattern. According to the estimated  $\hat{\nu}$  and  $\hat{\phi}_0$ , the ER can be further evaluated. When single photon events arrival time  $t$  satisfy (a)  $2n\pi - \pi/M < \Phi(t) < 2n\pi + \pi/M$  or (b)  $2n\pi + (M-1)\pi/M < \Phi(t) < 2n\pi + (M+1)\pi/M$ , a valid event is counted, where  $\Phi(t) = 2\pi\hat{\nu}t + \hat{\phi}_0$ . If condition (a) ((b)) is satisfied and  $D_0$  ( $D_1$ ) clicks, it is counted as a correct event. Otherwise, if condition (a) ((b)) is satisfied and  $D_1$  ( $D_0$ ) clicks, it is counted as an error event.

After the estimation, the first two terms of Equation 1 reduce to the estimation error in the analysis of the ER. While the third term (mainly contributed by the phase noise of laser source and the fiber length fluctuation) is a random noise, its contribution can be analyzed in theory and characterized in experiment. To do so, we derive an analytical model to study the phase noise/fluctuation and provide a guideline to optimize the experimental parameters. In previous TF-QKD experiments [7, 14, 16], the variance of fiber fluctuation of a fixed time interval is normally specified using time-domain measurements. In contrast, we use the *frequency-domain* power spectral density (PSD) to characterize the random noise. By doing so, we are able to calculate the fluctuation in variable interval  $\tau$  and relate it to the ER. Furthermore, the phase noise of the laser sources is also taken into consideration in our model. This was often ignored in the previous analysis for the phase-locked TF-QKD schemes [7, 14, 16]. Nonetheless, as the linewidth of the laser source increases, it will

dominate the phase fluctuation. Even for the phase-locked laser sources, their phase noise replicate the one of the reference source at best, which can not be ignored. By including the phase noise, our model can properly analyze the linewidth requirement for the laser sources for both phase-locking and no-phase-locking TF-QKD.

*Setup.*—To implement the no-phase-locking TF-QKD scheme, we build an experimental setup as shown in Fig. 2. Alice and Bob transmit their quantum light to Charlie’s measurement site via symmetric quantum channels, constituted by standard telecom fiber spools (G.652). No servo link is used for the dissemination of a third phase reference laser. Each user holds a commercial external cavity laser diode (RIO PLANEX) with a Lorentzian linewidth of 5 kHz and the wavelength is set at 1550.12 nm, but with a slight frequency mismatch of about 100 MHz. The frequency drifts slowly to an extent of 30 MHz over one day, which can be tracked by the frequency estimation algorithm.

The continuous light is encoded into two frames by three cascaded intensity modulators. Due to the fact that two lasers are heterodyned, no modulation in intensity and phase is required for the R-frame to resolve the phase ambiguity as in ref. [14, 16]. The Q-frame is used to generate quantum signals following the 3-intensity sending-or-not-sending (SNS) TF-QKD protocol [30]. Two cascaded phase modulators are used for 16-level random phase modulation covering  $2\pi$  range. One intensity modulator creates the two frames and modulates the weak decoy intensity, and the other two shape the pulses in Q-frame and extinct vacuum pulses jointly. Such configuration allow us to apply bias control on the first intensity modulator to stabilize the signal and decoy intensities.

Light from Alice and Bob interfere at Charlie’s 50:50 beam splitter with the same polarization as the output of the polarization beamsplitter is polarization-maintaining. This transforms the polarization variation into intensity variation. We use two electrical polarization controllers to rotate the polarization at 5 Hz so as to keep the photon rates at the other port of the polarization beamsplitter constant (5% of total photon rate). Moreover, the photons detected by  $D_2$  ( $D_3$ ) are accumulated to track the delay drift of the fiber every 5 s. The transition edge from the Q-frame to the R-frame is used as the time mark. These are sufficient to compensate the polarization and delay drift caused by the indoor fiber spools.

The interference output is detected by two superconducting nanowire single photon detectors (SNSPD). We use two types of SNSPDs, SNSPD#1 and #2, to perform the measurements. The detected photon events are registered by a time tagging unit and then processed

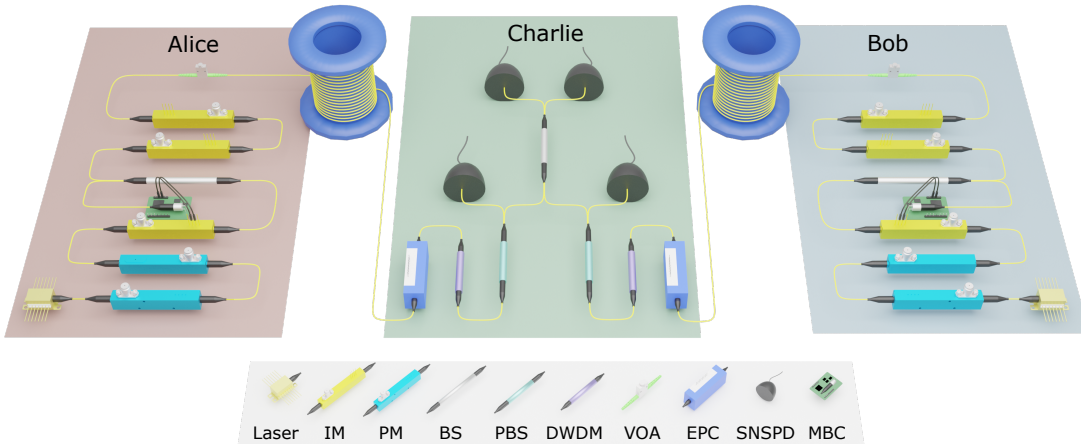


FIG. 2. Experimental setup. Alice (Bob) send their phase- and intensity-modulated states to Charlie to perform single-photon measurements.  $D_{0(1)}$  are used to generate secure keys, while  $D_{2(3)}$  are used for delay and polarization compensation. PM, phase modulator; IM, intensity modulator; BS, beamsplitter; VOA, variable optical attenuator; EPC, electrical polarization controller; DWDM, dense wavelength-division multiplexer; PBS, polarization beamsplitter; SNSPD, superconducting nanowire single photon detector; MBC, modulator bias controller.

by a computer. The frequency  $\hat{\nu}$  and initial phase  $\hat{\phi}_0$  of the beat note can be both estimated by the FFT-based algorithm. The valid arriving time  $t$  in X basis should satisfy:

$$\left| \cos \left( 2\pi\hat{\nu}t + \hat{\phi}_0 + (\phi_a - \phi_b) \right) \right| \geq \cos(\pi/16), \quad (2)$$

where  $\phi_a$  ( $\phi_b$ ) is phase modulated by the users and announced publicly in the post-processing. We also use actively odd-parity pairing method [31, 32] in the error rejection through two-way classical communication, significantly reducing the bit-flip error rate.

*Results.*—We firstly analyze the system performance with the no-phase-locking scheme quantitatively. The phase noise PSD of the laser has a -20 dB/decade slope, contributed by the white frequency noise. The phase noise PSD introduced by the fiber spool is also measured, which is mainly distributed below the frequency 100 kHz and increase slightly with the fiber length. With these two results, the phase fluctuation in the Q-frame can be calculated accordingly. The fluctuation is converted to the ER and averaged over the duration of the Q-frame.

To characterize the ER with different  $T_Q$  and  $T_R$ , we use the same setup as in Fig. 2, except that no modulation is applied. We plot measured ER as a function of  $T_R$  with different

photon count rates in Fig. 3a. A higher count rate enables accurate frequency estimation at smaller  $T_R$ , thus lowering the minimum ER. The simulation result assuming accurate frequency estimation is also plotted, including only the influence of the phase fluctuation. Based on these results and the constraint of the experimental system, we choose  $T_R$  and  $T_Q$  to be 4.9152 and 1.6384  $\mu\text{s}$  respectively. The ER contributes to the quantum bit error rate (QBER) of phase (X) basis in SNS-TF-QKD protocol. As another important implication of our theoretical model, we can determine the linewidth requirement for different selected  $T_Q$  and plot the simulated results in Fig. 3b. As an example, to achieve a maximum channel loss of 66 dB in our system, the laser linewidth should be narrower than 35.5 kHz when  $T_Q = 1 \mu\text{s}$ , resulting in an ER of 11%.

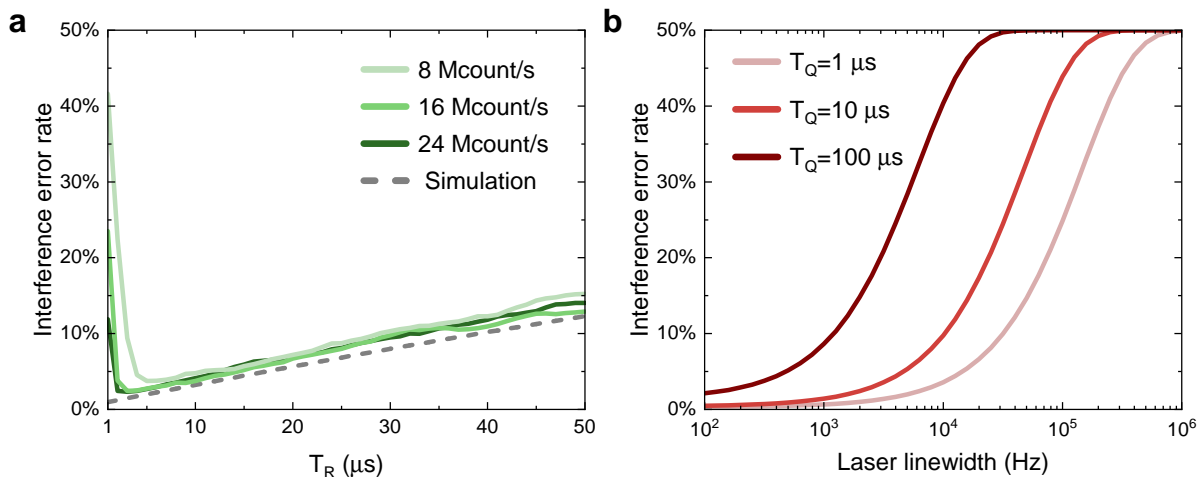


FIG. 3. **a**, Measured and simulated interference error rate as a function of  $T_R$  with different count rates per detector and  $T_Q = 1 \mu\text{s}$ . The simulated results assume accurate estimations. **b**, Interference error rate as functions of the laser linewidth and  $T_R = 5 \mu\text{s}$ , in which accurate estimation is also assumed.

With the performance analysis and parameter optimization, we perform TF-QKD experiments from 50 to 504-km standard fiber spools with different detectors and finite sizes. The channel is symmetrical and the total channel loss amounts to 9.6, 38.4, 56.8, 72.1 and 96.8 dB respectively. The results are presented in Fig. 4. With SNSPD#1, we measure the dynamic range to be 44 dB when the count rate of the R-frame is 24 Mcount/s and the duty cycle (i.e., the ratio of Q-frame) is 1/4. That is to say the dynamic dark count rate [33, 34] is about 1000 count/s, which is the dominant noise. To increase the signal-to-noise ratio,

we apply a gating window of 200 ps, resulting in a dark count probability of  $2 \times 10^{-7}$ . With less than one hour of continuous run, we achieve a finite-size SKR of  $1.25 \times 10^{-7}$  bit/pulse, or 39 bit/s at 380-km standard fiber. At the short end, we increase the duty cycle to 3/4. And it enable a secret key rate of 1.27 Mbit/s at 50-km standard fiber channel with a small number of sending pulses of  $10^{10}$ .

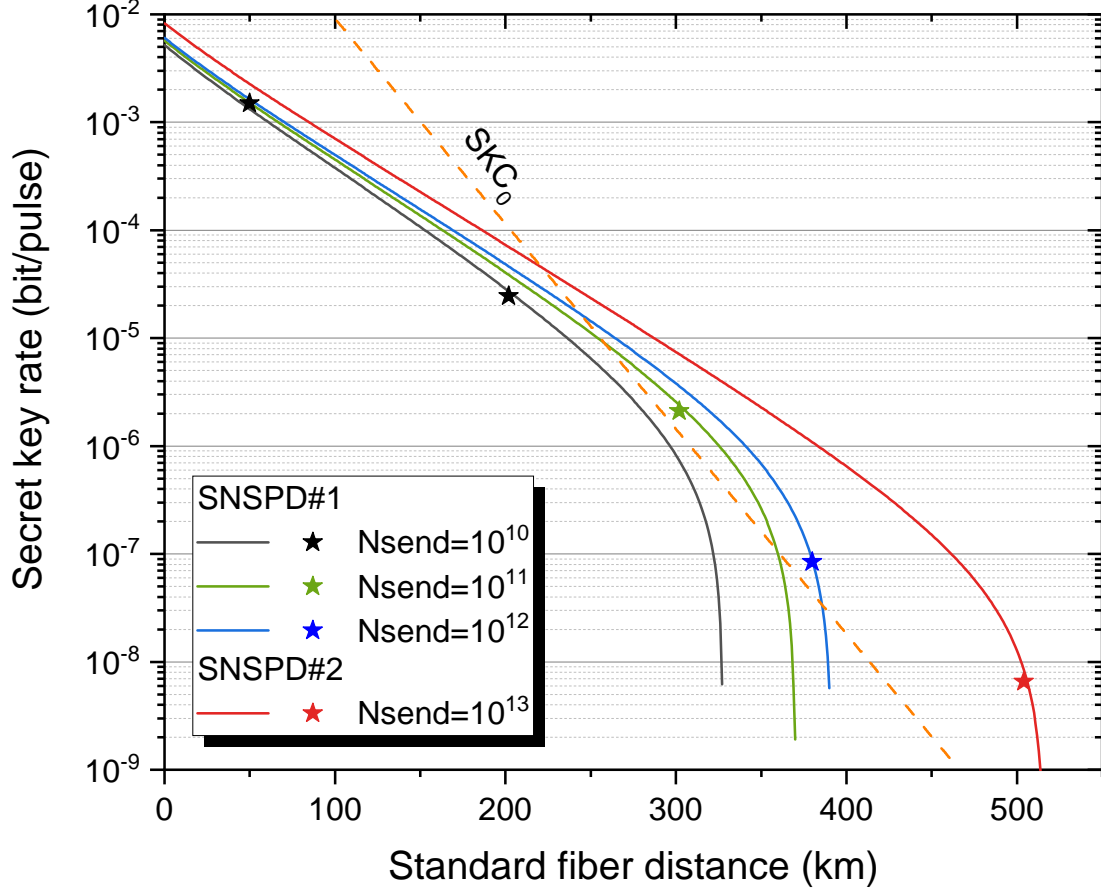


FIG. 4. SKRs at different standard fiber distances. The solid line is the simulated SKRs with different finite sizes and two sets of experimental parameters. The fiber loss coefficient is 0.19 dB/km. The solid stars denote the experimental results. The orange dashed line denotes  $SKC_0$ .

To generate positive key rates at longer distance, we replace the detectors with SNSPD#2, which has a dynamic range over 58 dB. Furthermore, we keep the detected count rate in R-frame as low as possible (8 Mcounts/s per detector) and use a narrower gating window of 100 ps. With these upgrades, the scattering noise in fiber becomes dominant and results



in a noise probability of  $1.6 \times 10^{-8}$ . This is an order of magnitude of improvement over SNSPD#1, allowing us to achieve a SKR of  $6.56 \times 10^{-9}$  bit/pulse or 2.05 bit/s at 504-km standard optical fiber.

*Discussion.*—In summary, we have proposed and demonstrated the no-phase-locking scheme for TF-QKD. Our scheme does not only remove the service channels for the dissemination of the reference light, but also does not need active phase compensation setup at the measurement site. Such features greatly simplify the setup to match the one of measurement-device-independent QKD systems [35, 36], with the ability to establish global phase reference nonetheless. We also show that commercial kilohertz linewidth semiconductor lasers are sufficient to perform TF-QKD with our scheme. Arguably, the simplification of setup with our scheme does not lead to performance degradation. With ultra-low-loss fiber deployed, 96.8-dB channel loss corresponds to over 600-km total distance, comparable to the state-of-art TF-QKD experiment with phase-locking sources [20] or phase-compensating module [18]. To achieve further transmission distance, one could increase the dynamic range of the SNSPD and insert a cryogenic bandpass filter to reduce the noise floor introduced by the background radiation. On the other hand, more advanced algorithm may require less counts in the recovery of the carrier, which helps to reduce the strong reference light intensity. Overall, we believe our scheme provides a practical solution to TF-QKD network and the phase recovery algorithm is applicable to other phase-sensitive applications [37, 38].

*Note added.*— While preparing the manuscript, we notice two related works which demonstrate different approaches [39, 40] to solve the phase-locking issue. Ref. [39] uses the modeparing MDI-QKD protocol and Ref. [40] employs the optical frequency comb. In contrast, we propose an efficient method to reconcile the phase reference in TF-QKD via data post-processing, and demonstrate high-rate TF-QKD and beat the repeaterless secret key capacity with two unlocked, low-cost, chip-scale lasers.

*Acknowledgement.*— This work was supported by National Natural Science Foundation of China (Grant No. 62031024, No. 12204467), Innovation Program for Quantum Science and Technology (2021ZD0300300), Anhui Initiative in Quantum Information Technologies, Shanghai Municipal Science and Technology Major Project (Grant No. 2019SHZDZX01), Shanghai Science and Technology Development Funds (22JC1402900) and Shanghai Academic/Technology Research Leader (21XD1403800). Y.L. acknowledges support from the Taishan Scholar Program of Shandong Province. F. Xu acknowledges the support from the

- [1] C. H. Bennett and G. Brassard, Quantum cryptography: Public key distribution and coin tossing, in *Proceedings of the IEEE International Conference on Computers, Systems, and Signal Processing* (1984) pp. 175–179.
- [2] F. Xu, X. Ma, Q. Zhang, H.-K. Lo, and J.-W. Pan, Secure quantum key distribution with realistic devices, *Rev. Mod. Phys.* **92**, 025002 (2020).
- [3] S. Pirandola, U. L. Andersen, L. Banchi, M. Berta, D. Bunandar, R. Colbeck, D. Englund, T. Gehring, C. Lupo, C. Ottaviani, J. L. Pereira, M. Razavi, J. S. Shaari, M. Tomamichel, V. C. Usenko, G. Vallone, P. Villoresi, and P. Wallden, *Advances in quantum cryptography*, [Adv. Opt. Photon.](#) **12**, 1012 (2020).
- [4] S. Pirandola, R. García-Patrón, S. L. Braunstein, and S. Lloyd, Direct and reverse secret-key capacities of a quantum channel, [Phys. Rev. Lett.](#) **102**, 050503 (2009).
- [5] M. Takeoka, S. Guha, and M. M. Wilde, Fundamental rate-loss tradeoff for optical quantum key distribution, *Nat. Commun.* **5**, 5235 (2014).
- [6] S. Pirandola, R. Laurenza, C. Ottaviani, and L. Banchi, Fundamental limits of repeaterless quantum communications, [Nat. Commun.](#) **8**, 15043 (2017).
- [7] M. Lucamarini, Z. L. Yuan, J. F. Dynes, and A. J. Shields, Overcoming the rate–distance limit of quantum key distribution without quantum repeaters, [Nature](#) **557**, 400 (2018).
- [8] H.-K. Lo, M. Curty, and B. Qi, Measurement-device-independent quantum key distribution, *Phys. Rev. Lett.* **108**, 130503 (2012).
- [9] X. Ma, P. Zeng, and H. Zhou, Phase-matching quantum key distribution, *Phys. Rev. X* **8**, 031043 (2018).
- [10] X.-B. Wang, Z.-W. Yu, and X.-L. Hu, Twin-field quantum key distribution with large misalignment error, *Phys. Rev. A* **98**, 062323 (2018).
- [11] M. Curty, K. Azuma, and H.-K. Lo, Simple security proof of twin-field type quantum key distribution protocol, *npj Quantum Inf.* **5**, 64 (2019).
- [12] C. Cui, Z.-Q. Yin, R. Wang, W. Chen, S. Wang, G.-C. Guo, and Z.-F. Han, Twin-field quantum key distribution without phase postselection, *Phys. Rev. Applied* **11**, 034053 (2019).
- [13] M. Minder, M. Pittaluga, G. Roberts, M. Lucamarini, J. Dynes, Z. Yuan, and A. Shields,

- Experimental quantum key distribution beyond the repeaterless secret key capacity, *Nat. Photonics* **13**, 334 (2019).
- [14] Y. Liu, Z.-W. Yu, W. Zhang, J.-Y. Guan, J.-P. Chen, C. Zhang, X.-L. Hu, H. Li, C. Jiang, J. Lin, T.-Y. Chen, L. You, Z. Wang, X.-B. Wang, Q. Zhang, and J.-W. Pan, Experimental twin-field quantum key distribution through sending or not sending, *Phys. Rev. Lett.* **123**, 100505 (2019).
- [15] S. Wang, D.-Y. He, Z.-Q. Yin, F.-Y. Lu, C.-H. Cui, W. Chen, Z. Zhou, G.-C. Guo, and Z.-F. Han, Beating the fundamental rate-distance limit in a proof-of-principle quantum key distribution system, *Phys. Rev. X* **9**, 021046 (2019).
- [16] X.-T. Fang, P. Zeng, H. Liu, M. Zou, W. Wu, Y.-L. Tang, Y.-J. Sheng, Y. Xiang, W. Zhang, H. Li, Z. Wang, L. You, M.-J. Li, H. Chen, Y.-A. Chen, Q. Zhang, C.-Z. Peng, X. Ma, T.-Y. Chen, and J.-W. Pan, Implementation of quantum key distribution surpassing the linear rate-transmittance bound, *Nat. Photonics* **14**, 422 (2020).
- [17] X. Zhong, J. Hu, M. Curty, L. Qian, and H.-K. Lo, Proof-of-principle experimental demonstration of twin-field type quantum key distribution, *Phys. Rev. Lett.* **123**, 100506 (2019).
- [18] M. Pittaluga, M. Minder, M. Lucamarini, M. Sanzaro, R. I. Woodward, M.-J. Li, Z. Yuan, and A. J. Shields, 600-km repeater-like quantum communications with dual-band stabilization, *Nat. Photonics* **15**, 530 (2021).
- [19] J.-P. Chen, C. Zhang, Y. Liu, C. Jiang, W.-J. Zhang, Z.-Y. Han, S.-Z. Ma, X.-L. Hu, Y.-H. Li, H. Liu, F. Zhou, H.-F. Jiang, T.-Y. Chen, H. Li, L.-X. You, Z. Wang, X.-B. Wang, Q. Zhang, and J.-W. Pan, Twin-field quantum key distribution over 511 km optical fiber linking two distant metropolitans, *Nat. Photonics* **15**, 570 (2021).
- [20] J.-P. Chen, C. Zhang, Y. Liu, C. Jiang, D.-F. Zhao, W.-J. Zhang, F.-X. Chen, H. Li, L.-X. You, Z. Wang, Y. Chen, X.-B. Wang, Q. Zhang, and J.-W. Pan, Quantum key distribution over 658 km fiber with distributed vibration sensing, *Phys. Rev. Lett.* **128**, 180502 (2022).
- [21] S. Wang, Z.-Q. Yin, D.-Y. He, W. Chen, R.-Q. Wang, P. Ye, Y. Zhou, G.-J. Fan-Yuan, F.-X. Wang, W. Chen, Y.-G. Zhu, P. V. Morozov, A. V. Divochiy, Z. Zhou, G.-C. Guo, and Z.-F. Han, Twin-field quantum key distribution over 830-km fibre, [Nat. Photon.](#) **16**, 154 (2022).
- [22] M. Peev, C. Pacher, R. Alléaume, C. Barreiro, J. Bouda, W. Boxleitner, T. Debuisschert, E. Diamanti, M. Dianati, J. Dynes, S. Fasel, S. Fossier, S. Fürst, J.-D. Gautie, O. Gay, N. Gisin, P. Grangier, A. Happe, Y. Hasani, M. Hentschel, H. Hübel, G. Humer, T. Länger,

- M. Legré, R. Lieger, J. Lodewyck, T. Lorünser, N. Lütkenhau, A. Marhold, T. Matyus, O. Maurhart, L. Monat, S. Nauerth, J.-B. Page, A. Poppe, E. Querasser, G. Ribordy, S. Robyr, L. Salvail, A. Sharpe, P. Trinkler, R. Tualle-Brouri, F. Vannel, N. Walenta, H. Weier, H. Weinfurter, I. Wimberger, Z. Yuan, H. Zbinden, and A. Zeilinger, The SECOQC quantum key distribution network in Vienna, *New J. Phys.* **11**, 075001 (2009).
- [23] M. Sasaki, M. Fujiwara, H. Ishizuka, W. Klaus, K. Wakui, M. Takeoka, S. Miki, T. Yamashita, Z. Wang, A. Tanaka, K. Yoshino, Y. Nambu, S. Takahashi, A. Tajima, A. Tomita, T. Domeki, T. Hasegawa, Y. Sakai, H. Kobayashi, T. Asai, K. Shimizu, T. Tokura, T. Tsurumaru, M. Matsui, T. Honjo, K. Tamaki, H. Takesue, Y. Tokura, J. Dynes, A. Dixon, A. Sharpe, Z. Yuan, A. Shields, S. Uchikoga, M. Legré, S. Robyr, P. Trinkler, L. Monat, J.-B. Page, G. Ribordy, A. Poppe, A. Allacher, O. Maurhart, T. Länger, M. Peev, and A. Zeilinger, Field test of quantum key distribution in the Tokyo QKD network, *Opt. Express* **19**, 10387 (2011).
- [24] Y.-A. Chen, Q. Zhang, T.-Y. Chen, W.-Q. Cai, S.-K. Liao, J. Zhang, K. Chen, J. Yin, J.-G. Ren, Z. Chen, S.-L. Han, Q. Yu, K. Liang, F. Zhou, X. Yuan, M.-S. Zhao, T.-Y. Wang, X. Jiang, L. Zhang, W.-Y. Liu, Y. Li, Q. Shen, Y. Cao, C.-Y. Lu, R. Shu, J.-Y. Wang, L. Li, N.-L. Liu, F. Xu, X.-B. Wang, C.-Z. Peng, and J.-W. Pan, An integrated space-to-ground quantum communication network over 4,600 kilometres, *Nature* **589**, 214 (2021).
- [25] G. Vallone, D. Bacco, D. Dequal, S. Gaiarin, V. Luceri, G. Bianco, and P. Villoresi, Experimental satellite quantum communications, *Phys. Rev. Lett.* **115**, 040502 (2015).
- [26] Y. Cao, Y.-H. Li, K.-X. Yang, Y.-F. Jiang, S.-L. Li, X.-L. Hu, M. Abulizi, C.-L. Li, W. Zhang, Q.-C. Sun, W.-Y. Liu, X. Jiang, S.-K. Liao, J.-G. Ren, H. Li, L. You, Z. Wang, J. Yin, C.-Y. Lu, X.-B. Wang, Q. Zhang, C.-Z. Peng, and J.-W. Pan, Long-distance free-space measurement-device-independent quantum key distribution, *Phys. Rev. Lett.* **125**, 260503 (2020).
- [27] C. Ma, W. D. Sacher, Z. Tang, J. C. Mikkelsen, Y. Yang, F. Xu, T. Thiessen, H.-K. Lo, and J. K. Poon, Silicon photonic transmitter for polarization-encoded quantum key distribution, *Optica* **3**, 1274 (2016).
- [28] P. Sibson, C. Erven, M. Godfrey, S. Miki, T. Yamashita, M. Fujiwara, M. Sasaki, H. Terai, M. G. Tanner, C. M. Natarajan, R. H. Hadfield, J. L. O’Brien, and M. G. Thompson, Chip-based quantum key distribution, *Nat. Commun.* **8**, 13984 (2017).
- [29] K. Wei, W. Li, H. Tan, Y. Li, H. Min, W.-J. Zhang, H. Li, L. You, Z. Wang, X. Jiang, T.-Y. Chen, S.-K. Liao, C.-Z. Peng, F. Xu, and J.-W. Pan, High-speed measurement-device-

- independent quantum key distribution with integrated silicon photonics, *Phys. Rev. X* **10**, 031030 (2020).
- [30] Z.-W. Yu, X.-L. Hu, C. Jiang, H. Xu, and X.-B. Wang, Sending-or-not-sending twin-field quantum key distribution in practice, *Sci. Rep.* **9**, 3080 (2019).
- [31] H. Xu, Z.-W. Yu, C. Jiang, X.-L. Hu, and X.-B. Wang, Sending-or-not-sending twin-field quantum key distribution: Breaking the direct transmission key rate, *Phys. Rev. A* **101**, 042330 (2020).
- [32] C. Jiang, X.-L. Hu, Z.-W. Yu, and X.-B. Wang, Composable security for practical quantum key distribution with two way classical communication, *New J. Phys.* **23**, 063038 (2021).
- [33] V. Burenkov, H. Xu, B. Qi, R. H. Hadfield, and H.-K. Lo, Investigations of afterpulsing and detection efficiency recovery in superconducting nanowire single-photon detectors, *J. Appl. Phys.* **113**, 213102 (2013).
- [34] S. Chen, L. You, W. Zhang, X. Yang, H. Li, L. Zhang, Z. Wang, and X. Xie, Dark counts of superconducting nanowire single-photon detector under illumination, *Opt. Express* **23**, 10786 (2015).
- [35] Y. Liu, T.-Y. Chen, L.-J. Wang, H. Liang, G.-L. Shentu, J. Wang, K. Cui, H.-L. Yin, N.-L. Liu, L. Li, X. Ma, J. S. Pelc, M. M. Fejer, C.-Z. Peng, Q. Zhang, and J.-W. Pan, Experimental measurement-device-independent quantum key distribution, *Phys. Rev. Lett.* **111**, 130502 (2013).
- [36] L. C. Comandar, M. Lucamarini, B. Fröhlich, J. F. Dynes, A. W. Sharpe, S. W.-B. Tam, Z. L. Yuan, R. V. Pentyl, and A. J. Shields, Quantum key distribution without detector vulnerabilities using optically seeded lasers, *Nat. Photonics* **10**, 312 (2016).
- [37] L.-M. Duan, M. D. Lukin, J. I. Cirac, and P. Zoller, Long-distance quantum communication with atomic ensembles and linear optics, *Nature* **414**, 413 (2001).
- [38] P. C. Humphreys, N. Kalb, J. P. J. Morits, R. N. Schouten, R. F. L. Vermeulen, D. J. Twitchen, M. Markham, and R. Hanson, Deterministic delivery of remote entanglement on a quantum network, *Nature* **558**, 268 (2018).
- [39] H.-T. Zhu, Y. Huang, H. Liu, P. Zeng, M. Zou, Y. Dai, S. Tang, H. Li, L. You, Z. Wang, *et al.*, Experimental mode-pairing measurement-device-independent quantum key distribution without global phase-locking, arXiv preprint arXiv:2208.05649 (2022).
- [40] L. Zhou, J. Lin, Y. Jing, and Z. Yuan, Twin-field quantum key distribution without optical

frequency dissemination, arXiv preprint arXiv:2208.09347 (2022).